IOP PUBLISHING NANOTECHNOLOGY
Nanotechnology **18** (2007) 115718 (7pp) doi:10.1088/0957-4484/18/11/115718

Simulating fullerene ball bearings of ultra-low friction

Xiaoyan Li[1] **and Wei Yang**[1,2]

[1] Department of Engineering Mechanics, Tsinghua University, Beijing 100084, People's Republic of China
[2] Zhejiang University, Hangzhou 310027, People's Republic of China

E-mail: yw-dem@tsinghua.edu.cn

Received 8 September 2006, in final form 8 January 2007
Published 14 February 2007
Online at stacks.iop.org/Nano/18/115718

Abstract
We report the direct molecular dynamics simulations for molecular ball bearings composed of fullerene molecules (C_{60} and C_{20}) and multi-walled carbon nanotubes. The comparison of friction levels indicates that fullerene ball bearings have extremely low friction (with minimal frictional forces of 5.283×10^{-7} and 6.768×10^{-7} nN/atom for C_{60} and C_{20} bearings) and energy dissipation (lowest dissipation per cycle of 0.013 and 0.016 meV/atom for C_{60} and C_{20} bearings). A single fullerene inside the ball bearings exhibits various motion statuses of mixed translation and rotation. The influences of the shaft's distortion on the long-ranged potential energy and normal force are discussed. The phonic dissipation mechanism leads to a non-monotonic function between the friction and the load rate for the molecular bearings.

(Some figures in this article are in colour only in the electronic version)

1. Introduction

Exploring tribological properties at the atomic scale is a fascinating and challenging enterprise. It leads to further understanding of the friction and energy dissipation, which will open up the possibility of designing and fabricating nanoscale machinery. Since Drexler [1, 2] proposed a model of molecular bearings, a great deal of theoretical, experimental and computational work has been performed to realize a frictionless microsystem alluded to by Feynman [3]. During the early studies, the symmetry [4] and superrotary [5] properties were investigated via rigid-body and semi-classical dynamics. Cumings and Zettl [6] were the first to observe telescopic extension and retraction of multi-wall carbon nanotubes (MWCNTs) without wear and fatigue. Yu *et al* [7] quantified the sliding frictional force as approximately 7.5×10^{-5} nN/atom between nested shells by pulling out the internal shells of the MWCNTs. The theoretical and experimental studies [8, 9] indicate that the MWCNTs can serve as low-friction and low-wear nanobearings. When the registry-dependent interactions are completely suppressed, the defect-free MWCNTs can become 'smoothest bearings' [9, 10]. Recently, Kis *et al* [11] experimentally estimated that the interlayer force is below 1.4×10^{-6} nN/atom for MWCNTs with stable defects. This result implies that the MWCNTs have a self-healing ability to optimize the atomic structure and preserve the absence of detectable mechanical dissipation. Atomistic simulations [12, 13] also showed that a double-walled carbon nanotube (DWCNT) bearing has extremely small frictional coefficient.

These previous investigations refer to molecular bearings with sliding surface friction. From the tribological point of view, the ball bearings may attain even lower friction levels ascribing to the rolling friction. Fullerene molecules, especially C_{60}, possess unique lubrication effects, and they have been treated as a lubricant [14] due to their near-perfect spherical shape. Therefore, Miura and Kamiya [15] constructed an ultra-lubricated molecular ball bearing by confining a C_{60} monolayer between graphite sheets. They explained the observed low frictional force via a stick–slip rolling model. Inspired by this experiment, many studies have focused exclusively on the energy dissipation mechanism during microscopic rolling. Braun [16] accomplished a two-dimensional molecular dynamics (MD) simulation which showed the relations between the rolling friction and lubricant concentration. The effect of C_{60} rotation on the nanotribology of C_{60} surfaces has been studied by atomic/frictional force microscopy [17]. The corresponding results revealed that

the free rotation of C_{60} caused an abrupt change in adhesion but a less obvious change in friction [17]. However, Coffey and Krim [18] reported the experimental observation of increased friction for the case of rapid rotation. Moreover, Legoas *et al* [19] reported that the stick–slip rolling was not observed during MD simulations for C_{60} nanobearings. Kang and Hwang [20] discussed the application of endo-fullerene molecules in the ball bearings. Depending on the precise chemical synthesis, a variety of molecular machines related to bearings have been developed and manufactured. Kelly *et al* [21] have synthesized a solution-phase molecular rotor controlled by the ion concentration. A surface-capable molecular nanocar [22], the world's smallest car, has been designed and constructed. It was observed that the movement of nanocars is a new type of fullerene-based wheel-like rolling motion [22]. Recently, a motorized nanocar has been synthesized by bearing a light-powered molecular motor [23]. The rotor–stator molecular crystals have been prepared from aromatic solutions of fullerenes and cubane [24].

In this work, we investigated the friction levels of ball bearings composed of MWCNTs and C_{20}/C_{60} fullerenes by MD simulations. The frictional force was estimated by measuring the energy dissipation rate of the system. It is found that the fullerenes inside ball bearings exhibited various motion states and rotational behaviours. We compared the tribological properties of ball bearings with those of DWCNT bearings, and analysed the energy dissipation mechanisms in molecular bearings.

2. Methodology

As shown in figure 1, a ball bearing is modelled by encapsulating fullerene molecules between the inner and the outer tubes. The inner tube acts as the shaft, and the fullerenes as the balls. As the sleeve of the bearing, two outer tubes can resist the wavy deformation induced by fullerene vibration. The C_{60} bearing contains 80 fullerenes and three CNTs of chiralities (15, 1)/(42, 11)/(54, 6), summing up to 14 815 carbon atoms. And there are 9090 atoms in a C_{20} bearing with 120 fullerenes and concentric (15, 1)/(35, 7)/(40, 13) nanotubes. Owing to the cylindrical confinement from the shaft and sleeve, the fullerenes are expected to form a certain ordered phase to preserve the optimal concentration of lubricant molecules. According to the literature [25, 26], fullerenes exhibit a helical structure in thick multi-walled nanotubes. So the initial arrangement of fullerenes in the bearing has a representative helical characteristic. The C_{60} and C_{20} bearings have lengths of 8.0 and 7.0 nm, respectively. The distances from the centre of C_{60} and C_{20} to that of the inner tube are 1.25 and 1.07 nm, respectively. Notably, the C_{20} fullerene is considered to be unstable under ambient conditions because of its extreme curvature and reactivity [27]. On the basis of highly accurate calculations [28, 29] and experiments [30], it is demonstrated that C_{20} fullerene survives for at least a short time (within the measurable time scale, which is considerably longer than the time scale of MD simulations). Under this limitation, the employment of C_{20} fullerene as the ball in molecular bearings is only an academic idealization.

In a molecular ball bearing, the forces on atoms include short- and long-ranged interactions. The short-ranged

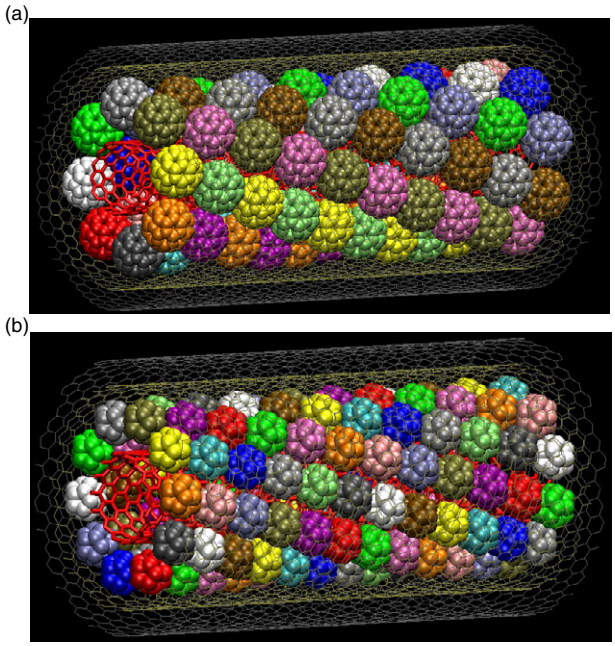

Figure 1. The molecular ball bearings composed of fullerenes and multi-walled nanotubes: (a) C_{60} @ (15, 1)/(42, 11)/(54, 6); (b) C_{20} @ (15, 1)/(35, 7)/(40, 13).

interaction means carbon–carbon covalent bonding. In all of the MD simulations, we use the many-body, reactive empirical bond-order potential (REBOP) [31] to characterize the covalent interactions. The REBOP allows for covalent bond breaking and forming with associated changes in atomic hybridization [31]. The long-ranged interaction is the steric and van der Waals (vdW) force between the non-bonded atoms. To accurately describe long-ranged interactions which dominate the physical features of ball bearings, we adopt the third generation (termed 'RDP2' in [32]) of registry-dependent graphitic potential developed by Kolmogorov and Crespi [9, 32]. This potential contains the two-body vdW attraction and exponential atomic-core repulsion due to the interlayer wavefunction overlap [32]. It has not only predicted the MWCNT corrugation against interlayer sliding and turbostratic staking of graphitic bilayers [32], but has also been applied to simulate DWCNTs' rotational bearing [13]. This potential is much more realistic and accurate than the Lennard-Jones potential for the interlayer interaction in graphitic structures [32].

To improve the computational accuracy and efficiency, we carried out MD simulations for fullerene ball bearings using the multiple time step algorithm [33]. The dynamical trajectories are integrated with the shorter and longer time steps of 0.5 and 1.0 fs, respectively. Prior to the MD simulations, geometrical optimizations were performed by using the conjugate gradient method. We imposed periodic boundary conditions along the axial direction of the nanotubes, and locked a few atoms in the middle portion of the outer tubes. First, the system was freely relaxed for 50 ps, to reach a dynamical equilibrium configuration. Subsequently, the rotational loading was imposed by displacing the constrained atoms in the middle of the inner tubes. Thus the rotational velocity was obtained from the given angular displacement at

each time step. For different loading rates, all MD simulations were terminated when the inner tubes rotated three circles with respect to the outer tubes.

To keep a canonical ensemble during simulations, the bearing system was coupled to a Berendsen thermostat [34], and thus maintained a room temperature of 300 K. By choosing a suitable coupling time constant, the kinetic temperature of the system fluctuated within 10 K of the desired temperature. Such techniques ensure an isothermal rotation of the system, and strengthen the global coupling between the internal constraints and the external heat bath. The Berendsen method has fine accuracy and stability [34], which facilitates the estimation of the frictional force.

Several ambiguities exist in the measurements for nanoscale friction. It is noted that recent experiment [15] recorded a unique friction force loop with positive and negative regions. Some MD simulations [16, 19, 20, 35] also show that the atomic frictional force fluctuates between positive and negative numbers, but its mean value tends to zero. To realistically describe the frictional force of the physical system, we adopt an energetic method proposed by Zhang *et al* [13]. The average frictional force can be estimated by measuring the dissipated energy which exchanges between the system and the heat bath.

To contrast the friction levels between the ball bearing and the cylindrical bearing, we also performed MD simulations for DWCNT bearings [13]. The latter consists of two CNTs with the chiralities (9, 9) and (22, 4), whose lengths are 8.0 and 7.0 nm, respectively. The boundary conditions are analogous to those in [13]. The other simulation details are the same as those of a ball bearing. It is noted that a (9, 9) CNT has a diameter of 1.220 nm, and the inner tube of a ball bearing has a diameter of 1.215 nm.

3. Results and discussion

Under a load rate of 0.05 rotations per picosecond (rot/ps), we investigated the variations of long-ranged potential energy, normal force, frictional force and dissipated energy with respect to rotation times for the ball and cylindrical bearings. Figure 2(a) shows the relations between the long-ranged potential energy of the shaft and rotations. The potential energy differences result from the distribution of the fullerene balls and the compactness of sleeve's structure. The interlayer potential energy of the DWCNT bearing agrees well with the results from [13]. The normal force on the shaft is plotted in figure 2(b). By averaging the normal force over all time steps, the obtained mean values for the (9, 9)/(22, 4), C_{60} and C_{20} bearings are 2.451×10^{-2}, 2.55×10^{-3} and 2.09×10^{-3} nN/atom, respectively. Due to stronger interactions from the taut structures, the average normal force of the (9, 9)/(22, 4) bearing is an order of magnitude higher than that of ball bearings (see figure 4(a)). The C_{60} molecule has pentagonal and hexagonal rings, whereas C_{20} has only pentagons. When the six-membered ring of the C_{60} molecule stacks on that of the inner tube, A–A or A–B stacking [32] forms and consequently strengthens the interactions between C_{60} and the shaft. But that special stacking does not form between C_{20} and the shaft, leading to a slightly lower normal force for the C_{20} bearing

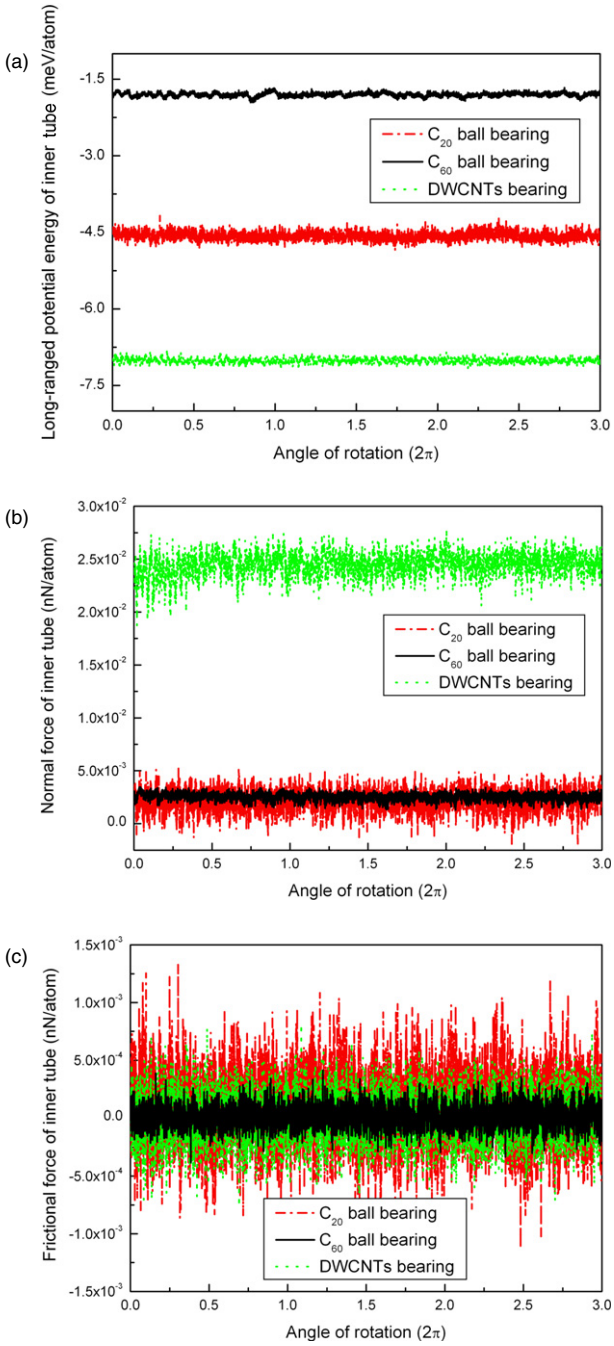

Figure 2. (a) Long-ranged potential energy, (b) normal force and (c) frictional force of the molecular bearings.

than that of the C_{60} bearing (see figure 4(a)). The dynamical frictional force profiles are shown in figure 2(c). There are positive and negative regions, but the mean values of the frictional force are almost zeros. Such observations are closely analogous to the experimental features [15].

Figure 3 shows the variations of dissipated energy versus the rotation time. For the DWCNT bearing, the dissipated energy fluctuates drastically at the initial stage of rotation. After that, it increases almost linearly with time, to indicate a steady state of the bearing system. In comparison, the C_{60} and C_{20} bearings have near-perfect linear energy dissipation. Based

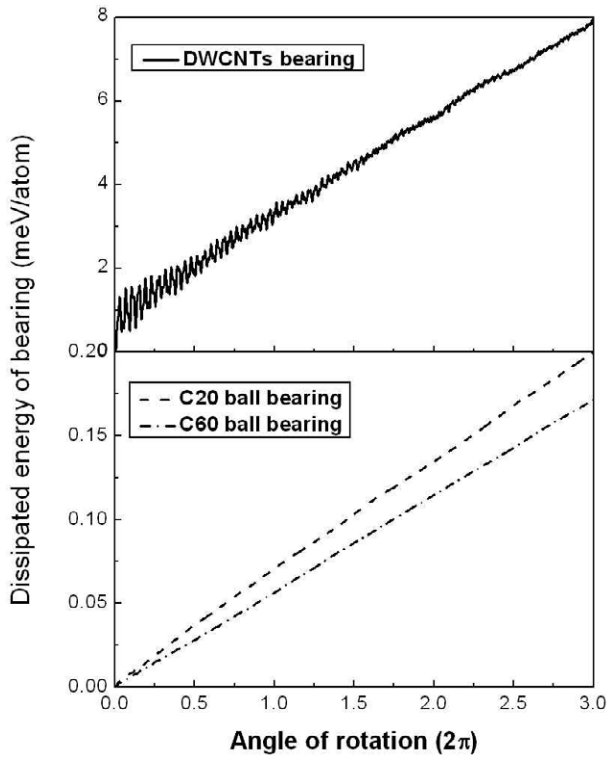

Figure 3. Dissipated energy of the molecular bearings.

on the steady variations of energy dissipation, one estimated that the total dissipated energy per cycle of the DWCNT, C_{60} and C_{20} bearings is 2.31, 0.057 and 0.066 meV/atom, respectively. This demonstrates that the rolling friction causes much lower and smoother energy dissipation than the sliding friction at the nanoscale. Furthermore, the C_{60} molecule is more effective than C_{20} for applications to molecular ball bearings.

The frictional coefficient of molecular bearings, as well as the energy dissipation rate, strongly depends on the loading rate [13]. To further investigate the dynamical effect, we imposed different loading rates on the shafts of all bearings. As shown in figure 4(a), the amplitude of the average normal forces initially remains constant, but it drops slowly with an increase of the loading rate. This phenomenon comes from the deformation or even failure of the shaft under a large loading rate. The average frictional forces for different loading rates are displayed in figure 4(b). The frictional forces of all bearings vary as a non-monotonic function of the loading rate. For relatively large rotational velocity, the shaft easily overcomes the energy barrier for rotation, leading to lower frictional heat. When the rotational velocity exceeds a critical value, the shaft may appear distorted or even collapsed, leading to high energy dissipation. Further interpretations related to phononic dissipation are given below. The dependence of frictional coefficient on the loading rate is delineated in figure 4(c). The minimal frictional coefficients of C_{60} and C_{20} bearings are 2.148×10^{-4} and 4.291×10^{-4}, corresponding to the friction forces of 5.283×10^{-7} and 6.768×10^{-7} nN/atom, and the energy dissipations per cycle of 0.013 and 0.016 meV/atom, respectively.

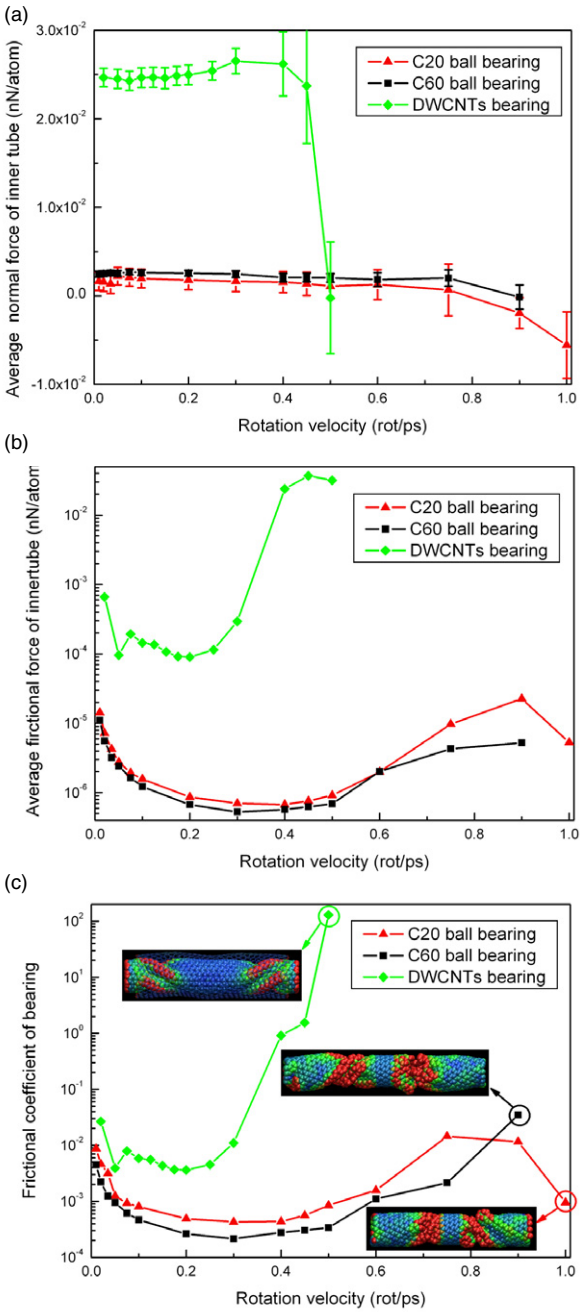

Figure 4. The variations of (a) average normal force, (b) average frictional force and (c) frictional coefficient with the rotation velocity for the molecular bearings. The graphs drawn in (c) show the failures of molecular bearings. The BGR scale in the graphs maps to total potential energy of atoms: blue represents lower energy, and red is higher energy.

For a single fullerene molecule, the translational and rotational kinetic energies are monitored during simulations. As shown in figure 5, each fullerene moves in a mixture of translation and rotation. A fullerene molecule inside the ball bearing may settle suddenly into a rapid rotation upon the thermal fluctuations [36], as a departure from constant rolling. Such rapid rotation is evidenced in figure 5(a), and absorbed by impacts with the neighbouring rolling molecules. Their collisions hinder the rapid rotation but destroy the smooth-

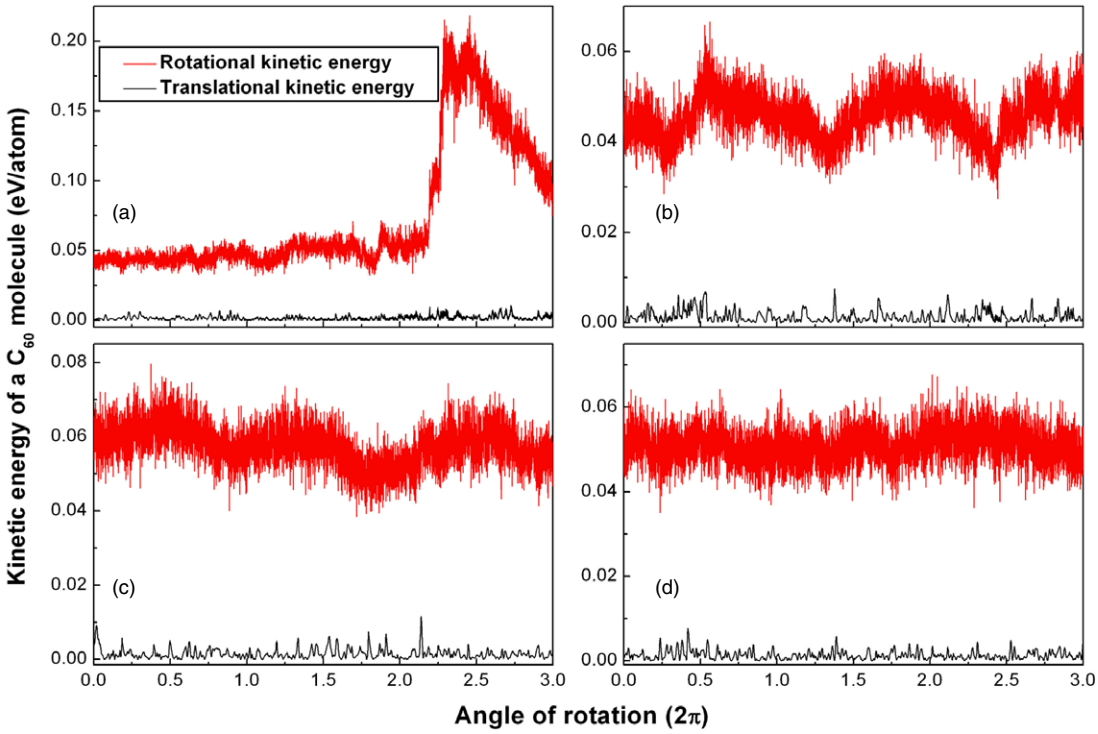

Figure 5. The motion states of a single fullerene molecule inside a C_{60} bearing.

rolling regime. Figures 5(b) and (c) show a motion state of periodic rolling. This response is a manifestation of the discrete step rotation which is similar to the stick–slip rolling suggested by Miura *et al* [15]. The peak of translational kinetic energy corresponds to thermal rotations, and the rest represents step rolling. Remarkably, the fullerene molecules are confined between curved faces of CNTs, instead of the graphite sheets in Miura's experiment [15]. As the shaft rotates, a fullerene may maintain constant rolling, synchronously accompanied by translation motion (see figure 5(d)). Aside from the above three motion states, the fullerene may exhibit rolling without distinct features. The rapid rotation can induce jamming or collision of lubricant molecules; therefore, it is obviously adverse for decreasing the friction. However, the periodic and constant rollings are energetically favourable in lowering the energy dissipation. Despite the above studies aimed at the C_{60} bearing, completely similar motion states are also observed inside a C_{20} bearing.

When the loading rate reaches a certain value, the imposed strain near the constrained atoms cannot be released with rotations. As a result, the radial distortion on the shaft is induced by accumulated strain. The distortion may gradually vanish with further rotation. From figures 6(a) and (b), it is seen in the C_{60} bearing that the long-ranged potential energy increases, but the normal force decreases during the shaft's distortion. After the shaft distortion disappears, the potential energy and normal force quickly tend to become stable. For the distorted DWCNT bearing, the sharp changes of the potential energy and normal force are illustrated in figure 6(c) and (d), respectively. When the loading rate is kept at 0.5 rot/ps, the potential energy and normal force cannot settle into a stable state after contortions. This implies that the shaft will collapse and the sleeve will corrugate (see figure 4(c)). Obviously, the (9, 9)/(22, 4) bearing fails at the loading rate of 0.5 rot/ps. On the other hand, the failures of C_{60} and C_{20} bearings occur at the rates of 0.9 and 1.0 rot/ps (see figure 4(c)), respectively. This indicates that the ball bearing has a broader work range than the cylindrical bearings.

So far it is widely recognized that the atomic friction is dominated by phonon and electronic excitations [37–42]. During all MD simulations for the molecular bearings, we employ a thermostat to establish statistical thermal equilibrium. Monitoring the energy exchange between the system and the thermostat bath allows us to focus on the system's dissipation due to phononic friction. For the molecular bearing, the non-monotonic relation between the friction and the loading rate can be explained by the phononic mechanism. The phonons are excited by the rotation of the shaft, and are sensitive to the rotation rate imposed by the constrained atoms. The rotation at a low velocity produces weak phononic friction for a long period, while the rotation at a high velocity generates strong phononic friction for a short period. Thus there exists a critical loading rate corresponding to the minimal energy dissipation. If the loading rate is above the critical value, the corrugation of the shaft and sleeve, or the jamming of lubricant molecules, will induce additional energy dissipation. For a molecular bearing at the atomic scale, the phononic excitation is a main energy dissipation mechanism.

4. Conclusion

In summary, we have studied the fullerene ball bearing using MD simulations. By contrasting the friction levels between the ball and cylindrical bearings, it is found that the molecular ball

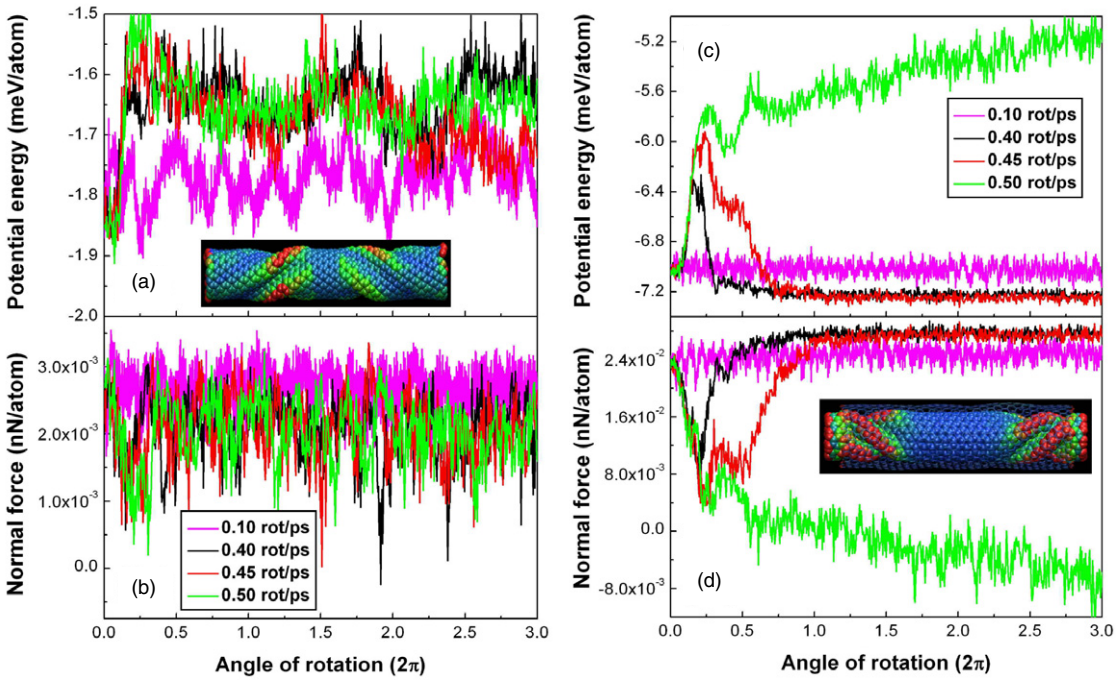

Figure 6. The influences of the shaft's distortion on the long-ranged potential and normal force for (a)–(b) C_{60} bearing, and (c)–(d) DWCNT bearing. The graphs drawn in (a) and (d) show the distortions of molecular bearings. The BGR scale still maps to total potential energy.

bearing has extremely low friction and much reduced energy dissipation. By analysing the variations of the kinetic energy with rotation time, a single fullerene molecule inside the ball bearing exhibits various motion statuses, such as rapid thermal rotation, and periodic and constant rolling. Furthermore, we have discussed the energy dissipation mechanism of the molecular bearings. The non-monotonic relation between the friction and the loading rate is interpreted by phononic excitations. It is noted that the density, uniformity and rotational behaviour of fullerene molecules are pivotal factors for controlling the friction levels of molecular ball bearings.

Acknowledgments

This work is sponsored by Grant Nos 10332020 and 10121202 from the National Natural Science Foundation of China, and also by Contract No. 2004CB619304 from the 973 Projects of China. We gratefully acknowledge the support of parallel computation on the HPCS supercomputer at the Chinese Academy of Meteorological Science.

References

[1] Drexler K E 1986 *Engines of Creation* (New York: Doubleday)
[2] Drexler K E 1992 *Nanosystems: Molecular Machinery, Manufacturing and Computation* (New York: Wiley)
[3] Feynman R 1960 *Eng. Sci.* **23** 22
[4] Merkle R C 1993 *Nanotechnology* **4** 86
[5] Sohlberg K, Tuzun R E, Sumpter B G and Noid D W 1997 *Nanotechnology* **8** 103
[6] Cumings J and Zettl A 2000 *Science* **289** 602
[7] Yu M F, Yabobson B I and Ruoff R S 2000 *J. Phys. Chem.* B **104** 8764
[8] Falvo M R, Tayor R M, Helser A, Chi V, Brooks F P, Washburn S and Superfine R 1999 *Nature* **397** 236
[9] Kolmogorov A N and Crespi V H 2000 *Phys. Rev. Lett.* **85** 4727
[10] Charlier J P and Michenaud J P 1993 *Phys. Rev. Lett.* **70** 1858
[11] Kis A, Jensen K, Aloni S, Mickelson W and Zettl A 2006 *Phys. Rev. Lett.* **97** 025501
[12] Tuzun R E, Noid D W and Sumpter B G 1995 *Nanotechnology* **6** 64
[13] Zhang S L, Liu W K and Ruoff R S 2004 *Nano Lett.* **4** 293
[14] Luthl R, Meyer E, Haefke H, Howald H, Gutmannsbauer W and Guntherodt H L 1994 *Science* **266** 1979
[15] Miura K and Kamiya S 2003 *Phys. Rev. Lett.* **90** 055509
[16] Braun O M 2005 *Phys. Rev. Lett.* **95** 126104
[17] Liang Q, Tsui O K T, Xu Y, Li H and Xiao X 2003 *Phys. Rev. Lett.* **90** 146102
[18] Coffey T and Krim J 2006 *Phys. Rev. Lett.* **96** 180104
[19] Legoas S B, Giro R and Galvao D S 2004 *Chem. Phys. Lett.* **386** 425
[20] Kang J W and Hwang H J 2004 *Nanotechnology* **14** 614
[21] Kelly T R, Bowyer M C, Bhaskar K V, Bebbington D, Garcia A, Lang F, Kim M H and Jette M P 1994 *J. Am. Chem. Soc.* **116** 3657
[22] Shirai Y, Osgood A J, Zhao Y, Kelly K F and Tour J M 2005 *Nano Lett.* **5** 2330
[23] Morin J F, Shirai Y and Tour J M 2006 *Org. Lett.* **8** 1713
[24] Pekker S *et al* 2005 *Nat. Mater.* **4** 764
[25] Hodak M and Girifalco L A 2003 *Phys. Rev.* B **67** 075419
[26] Troche K S, Coluci V R, Braga S F, Chinellato D D, Sato F, Legoas S B, Rurali R and Galvao D S 2005 *Nano Lett.* **5** 349
[27] Dollgonos G, Lukin O, Elstner M, Peslherbe G H and Leszczynski J 2006 *J. Phys. Chem.* A **110** 9405
[28] Taylor P R, Bylaska E, Weare J H and Kawai R 1995 *Chem. Phys. Lett.* **235** 558
[29] Saito S and Miyamoto Y 2001 *Phys. Rev. Lett.* **87** 035503
[30] Prinzbach H, Weiler A, Landenberger P, Wahl F, Worth J, Scott L T, Gelmont M, Olevano D and Issendorff B 2000 *Nature* **407** 60
[31] Brenner D W, Shenderova O A, Harrison J A, Stuart S J, Ni B and Sinnott S B 2002 *J. Phys.: Condens. Matter* **14** 783

[32] Kolmogorov A N and Crespi V H 2005 *Phys. Rev.* B **71** 235415
[33] Tuckerman M, Berne B J and Martyna G J 1992 *J. Chem. Phys.* **97** 1990
[34] Berendesn H J C, Postma J P M, van Gunsteren W F, DiNola A and Haak J R 1984 *J. Chem. Phys.* **81** 3684
[35] Harrison J A, White C T, Colton R J and Brenner D W 1992 *Phys. Rev.* B **46** 9700
[36] Johnson R D, Yannoni C S, Dorn H C, Salem J R and Bethune D S 1992 *Science* **255** 1235
[37] Krim J and Widom A 1988 *Phys. Rev.* B **38** 12184
[38] Cieplak M, Smith E D and Robbins M O 1994 *Science* **265** 1209
[39] Sokoloff J B 1995 *Phys. Rev.* B **52** 5318
[40] Cieplak M, Smith E D and Robbins M O 1996 *Phys. Rev.* B **54** 8252
[41] Tomassone M S, Sokoloff J B, Widom A and Krim J 1997 *Phys. Rev. Lett.* **79** 4798
[42] Torres E S, Goncalves S, Scherer C and Kiwi M 2006 *Phys. Rev.* B **73** 035434